AWESW2022
21st Australasian Wind Engineering Society Workshop
2 – 3 February, 2023

Effects of Turbulence and Building Geometry on Cladding Design Pressures

Gregory A. Kopp[1]
[1]*Boundary Layer Wind Tunnel Laboratory, Faculty of Engineering, Western University, London, ON, Canada.*

ABSTRACT

The performance of cladding, connections, and other building components is critical for reducing losses due to severe storms. Design wind loads for cladding and building components are typically obtained via the wind tunnel method or from codes and standards, which rely on wind tunnel data in their development. The determination of design wind loads for these systems is challenging, particularly for systems that are air permeable. Small air gaps between adjacent components and layers cannot be modeled at the typical scales used in boundary layer wind tunnels, which requires relaxation of the usual wind tunnel scaling laws for accuracy. The paper reviews recent advances in the understanding of building aerodynamics in regions of separated reattaching flow near building edges, focussing on the roofs of low-rise buildings as an illustrative example. Based on this, existing design standards and wind tunnel test methods are examined, with recommendations for developments to ensure both improved performance-based design and disaster resilience of these systems.

1. Introduction

It is now well known that economic losses in disasters caused by wind storms are closely related to the performance of cladding systems and the connections used with various building components. For single-family residential structures, which are often the driver for losses in severe storms, modern building codes have eliminated many of the structural performance issues (Gurley and Masters, 2014). However, cladding performance remains a significant source of losses, which are often amplified by rainwater entry (Sparks et al., 1994).

Cladding systems are often complex with multiple layers, many of which are air permeable. They are typically designed to control heat and moisture flows, with architectural considerations understandably given priority. Actual performance, of course, depends on both the loads and the resistance, and building codes and design standards cover both aspects. Because of the complexity, wind loading standards, such as ASCE 7-22 (2022), tend to treat cladding as being of a single, air-tight layer with external and internal pressure coefficients provided for a range of building shapes and openings. Details of the load sharing and pressure equalization through the multiple layers are usually dealt with in product testing standards (e.g., ASTM D3679, 2013; ASTM D5206, 2013). This approach is rational, since the particular details for different systems can be handled systematically, and usually leads to conservative (i.e., safe) results (although there are sometimes inconsistencies in how different products are treated in different standards).

With the rise of performance-based design on the one hand, and the need to mitigate the ever-rising losses caused by severe storms on the other, there are many issues that need to be addressed with respect to the design and performance of cladding systems. Performance-based design relates to the optimization of the performance goals and is, in essence, related to customizing both the design loads and resistance. This usually implies reducing the wind loads from those in codes and standards by

specialized analysis. Wind engineering consulting firms have been involved with this for decades through the wind tunnel method for determining wind loads on high-rise buildings. More recently, this has been through applying the wind tunnel method for the determination of wind loads on products, such as roof-mounted solar arrays (Banks, 2013). In contrast, there is a societal need to reduce the losses from wind-related disasters. While rising losses are often associated with rising populations in risk-prone areas and changing climatic patterns and intensity of storms, there are also detailed knowledge gaps that need to be addressed with respect to performance of cladding and building components in wind storms. There is need to ensure that product design and implementation is optimized to keep costs in check as society adapts to these changing circumstances.

Knowledge gaps related to the performance of cladding systems and building components include issues relate to (i) wind load standards (e.g., ASCE 7-22), (ii) product test standards (e.g., ASTM D5206), and (iii) wind tunnel test methods. The objective of the paper is to review the methods for the development of design values of the aerodynamic (i.e., area-averaged pressure) coefficients for cladding and component (C&C) systems. Due to space limitations and noting that wind tunnel data is the primary method for setting design loads, this presentation will only consider issues related to wind load standards and wind tunnel test methods. The paper will not examine the emerging issues associated with considerations of non-synoptic storms, such as tornadoes, although some of the methods discussed here are relevant for such storms. Only suctions near the edges of low-rise building roofs will be discussed. The large loads in these zones highlight the important issues, and it is noted that there is a clear analog in the separated flows causing the suctions on low-rise roofs and near the edges of high-rise building walls (as discussed in Liu et al., 2019; Wang and Kopp, 2022).

2. Review of Building Aerodynamics in Regions of Separated Reattaching Flow

Low-rise buildings are defined as having a roof height that is less than the least horizontal (plan) dimension. The flow field near roof edges of low-rise buildings is dominated by the separated flow, which tends to reattach onto the roof surface for these shapes (for nearly flat roofs). The largest suctions on the roof occur near the corner of the roof but are also high along all edges in the region of separated flow near the edge. There are two forms of the vortices in the flow field: one being the "corner" (also called "delta wing") vortices that originate from the corner for oblique wind directions, the other being the separation bubble for winds normal to the wall (when the flow reattaches). Peak pressures are closely related to these vortices (Saathoff and Melbourne, 1997; Banks and Meroney, 2001; Pratt and Kopp, 2014). The size of these vortices depends on the wall size, primarily the building height, as discussed in Lin and Surry (1998), Akon and Kopp (2016), and Kopp and Morrison (2018). Thus, the reattachment length, X_r, is a good proxy for the size of these vortices (Pratt and Kopp, 2014; Akon and Kopp, 2016), while the reattachment length depends on the height of the building, in particular the vertical distance on the windward wall from the stagnation point to the roof edge, h_f (Lin and Surry, 1998; Akon and Kopp, 2016). Hence, the region of high suction depends primarily on the height, H, of the low-rise building. In fact, the roof height is dominant geometric parameter for defining wind loads on low-rise buildings (Wang and Kopp, 2021).

Turbulence also plays an important role on the pressures in the region of separated flow. For simplicity, we will discuss the role of turbulence in terms of its scale, using the integral length scale of the longitudinal component (i.e., horizontal component in the nominal wind direction), L_x, and intensity, I_u. The reattachment length depends on both the scale and intensity of the turbulence (Saathoff and Melbourne, 1997). For low turbulence levels, the reattachment length is relatively large, being approximately $10h_f$ (Akon and Kopp, 2016). At the turbulence intensities and scales typical of open and suburban terrains, for typical low-rise building sizes, the reattachment length is fairly constant at about $4h_f$, which translates to about 1.0 to 1.5H for typical low-rise building shapes (Akon and Kopp, 2016).

In addition to altering the reattachment length, the turbulence alters the nature of the pressure fluctuations (and peak suctions) within the region of separated flow. For low turbulence upstream, the highest fluctuations are near the reattachment point due to impinging separated shear layer (SSL) at reattachment (Cherry et al., 1984; Saathoff and Melbourne, 1997). Turbulence grows as the flow moves downstream within the SSL, primarily due to the Kelvin-Helmholtz instability (Lander et al., 2018). The upstream turbulence alters the transition to turbulence in the separated shear layer, causing a bypass transition, which alters the nature of vortices and instabilities in the separated shear layer (Lander et al., 2016). For turbulence levels in typical open or suburban terrains, and typical low-rise building sizes, the separated shear layer is essentially fully turbulent right from separation, after which it immediately starts to decay (Akon and Kopp, 2018). For these turbulence levels, the aerodynamic mechanisms are essentially fixed and constant, such that the aerodynamic coefficients for area-averaged roof pressures do not change significantly with the terrain (Wu and Kopp, 2018).

Of some importance is the turbulence energy levels and critical frequencies that lead to the change of location of peak pressure fluctuations from the reattachment point to the roof edge. Melbourne (1979) identified that the critical frequencies should be related to the thickness of the SSL, which is on the order of 1/10 the height of the building, H. Putting this into a non-dimensional form implies that the critical frequency, $f^* = fH/V \sim 10$. Recent experiments with a low-rise building at H = 4m and Re = 3.2×10^6 led Morrison and Kopp (2018) to the conclusion that the range of frequencies, $0.1 < f^* < 2$, are active in controlling the SSL and the high fluctuations immediately adjacent to the roof edge. Thus, to obtain pressure coefficients that accurately represent those in full scale, matching the power spectral densities within this range is critical.

3. External Pressure Coefficients for C&C Design in ASCE 7

In 2016, ASCE 7 had a significant update of the pressure coefficients for roofs of low-rise buildings using the wind tunnel in Ho et al. (2005) and Vickery et al. (2011). The update considered about 60 building geometries ranging in size from those of single-family residential structures (i.e., houses) to reasonably large industrial buildings (i.e., warehouses), in two terrain conditions. Figure 1 shows the spatial layout of worst pressure coefficients, enveloped over wind direction for two buildings of the same plan dimensions but with different heights. The results show that the same patterns occur, although the spatial extent of the patterns clearly depends on the roof height. Based on this, Morrison and Kopp (2018) recommended zone sizes as a function of H, which are shown in Figure 2. Scaling the zones with H implies that the relative areas of the zones change as a function of the plan dimensions of the roof. So, for buildings that are close to a cube shape, there are only 2 zones, defined by the corner (zone 3) and edge (zone 2). For buildings with plan dimensions that are large relative to height, there are 4 zones. The detailed analysis for low-slope roofs can be found in Kopp and Morrison (2018).

To develop the pressure coefficients in 2016 version of ASCE 7, an enveloping procedure, whereby the worst values in a particular roof zone, regardless of wind direction, was used. In other words, using the pressure coefficients in Figure 1, the worst values in each zone for each building were obtained. These values were then plotted for each building and each zone and a curve fit was developed. Figure 3 depicts the results for the corner (zone 3), which show the peak area-averaged pressure coefficients, GCp, as a function of dimensional area, A_e, along with the code values. The figure shows that while all of the data show similar trends, there is a range of scatter. Given that the peak pressures are functions of the vortices in the separated reattaching flow above the roof, which scales with the height of the building, one might expect that the size of the building should alter area-averaged pressures in such a way that, for a fixed dimensional area, larger suctions should be observed for buildings with larger H. In fact, Lin and Surry (1998) suggested that the there may be a single curve for pressure coefficients plotted as a function of A_e/H^2. To examine this further, Doddipatla et al. (2022) tested a building with dimensions, H x W x L = 50m x 196m x 400m in the low-speed side of Western's Boundary Layer Wind

Tunnel 2. These authors confirmed the finding of Lin and Surry (1998) for this large low-rise-shaped building, with results for the roof corner (zone 3) shown in Figure 4.

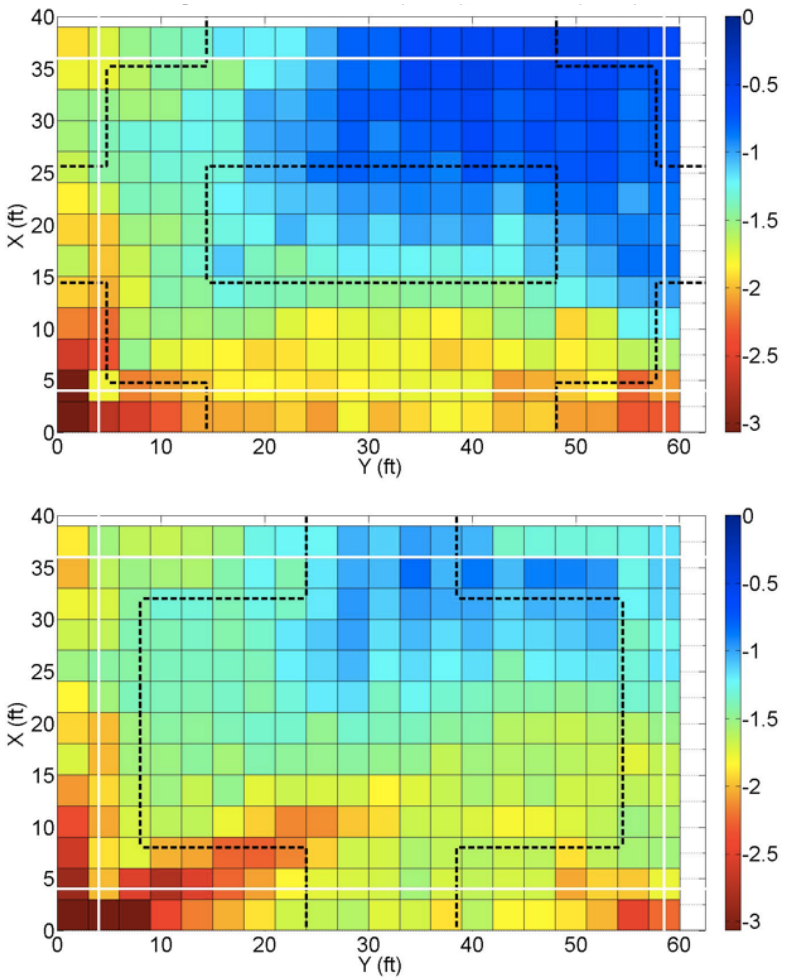

Figure 1. Spatial variation of worst peak pressure coefficients for area averages of 9ft^2 on buildings with plan dimensions of 40 ft x 62.5 and roof heights of (top) 24 ft and (bottom) 40 ft, in open terrain.

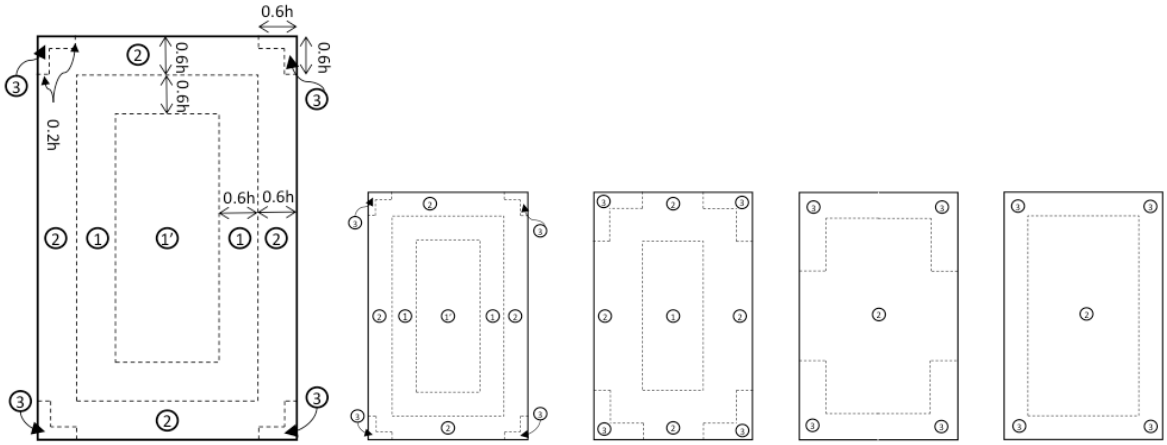

Figure 2. (Left) Roof zones for low-rise buildings with low-slope roofs used in ASCE 7-16. (Left-center) $L/H > 2.4$, (center) $1.2 < L/H < 2.4$, (right-center) $L/H < 1.2$ and $W/H > 1.2$, and (right) $L/H < 1.2$ and $W/H < 1.2$.

Given the exponential drop in the design pressure coefficients as a function of A_e, along with the dependence on building size, development of non-dimensional pressure coefficients would seem

reasonable, particularly for elements with small tributary areas. Since most cladding systems have multiple fasteners per panel, neglecting load sharing and using geometric tributary areas typically ensures a conservative design, (perhaps) offseting the under-estimated peak coefficients for relatively small areas on larger buildings. For example, for wood roof sheathing panels, Szilagyi (2022) found an effective area of about 24ft^2 for fasteners with geometric tributary areas of between 0.5 and 2ft^2 such that many fasteners participated in the failure at the limit state rather than the single fastener that is typically assumed for design. This is a concept that needs further investigation because it implies over-design on some buildings and under-design on others and is panel and fastener dependent. The use of non-dimensional effective wind areas, A_e, has been implemented for roof-mounted solar arrays in ASCE 7 (see Kopp, 2014, for a discussion), although methods for the determination of the correct value of A_e to use with racking systems have not yet been agreed on.

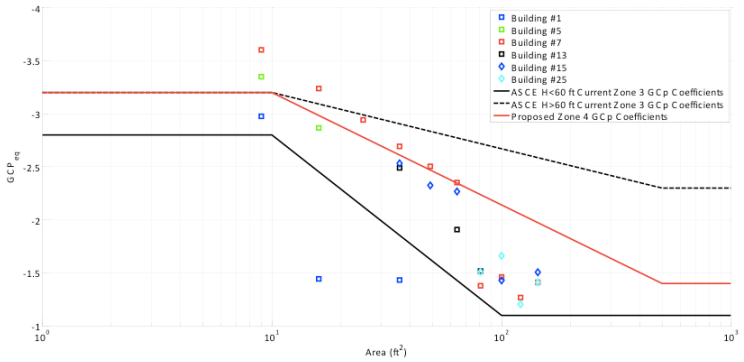

Figure 3. Peak enveloped pressure coefficients, *GCp*, as a function of area (ft^2) in the roof corner of ASCE 7.

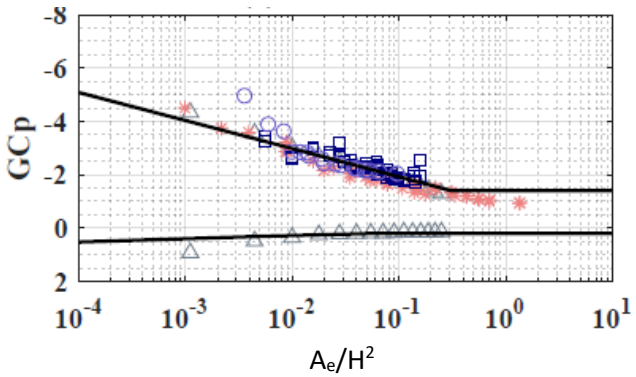

Figure 4. Peak enveloped pressure coefficients, *GCp*, as a function of non-dimensional area (A_e/H^2) in the roof corner zone of ASCE 7 with data from Kopp and Morrison (2018), Lin and Surry (1998), and a building with plan dimensions of 400m x 196m and a roof height of 50m (Doddipatla et al., 2022).

4. Wind Tunnel Method for Determining C&C Design Coefficients

While the wind tunnel method is well established for determining wind loads on complete structures, determining wind loads on relatively small building elements, especially when they have multiple layers is still an area of active research. There are challenges with determining wind loads on small cladding elements that are air permeable, since small gaps, which are critical to setting the net wind load, cannot be manufactured at typical the model scales of 1/200 to 1/500 used in boundary layer wind tunnels. Some of these, like discrete metal roofs (Miller et al., 2020), clay and concrete tiles (Smith, 2014), asphalt shingles, or wall siding products (Miller et al., 2017), may not even be able to be modelled at relatively large scales, e.g., 1/10, and may require full-scale experiments to determine wind loads. Figure 5 depicts the issue of gap size for concrete tiles from Smith (2014). The most common method to determine wind loads in this situation is called Partial Turbulence Simulation (PTS).

PTS is based on the aerodynamic concepts reviewed earlier, particularly that the relatively small scales (high frequencies) of turbulence control the flow patterns and aerodynamic loads. It is these scales that are required to accurately model the flow so that the aerodynamic coefficients can be obtained (Irwin, 2008; Banks, 2011; Morrison and Kopp, 2018). Essentially, the requirements are to simulate the turbulence spectrum is accurate over the range of frequencies that control the flow patterns around the building, which are usually given as $f^* > \sim 0.1$. One example is depicted in Figure 6, from the experiments reported by Stenabaugh et al. (2015) at a length scale of 1/20, using the direct measurement approach (Banks, 2011). ASCE 49-21 (2021), which governs the requirements for wind tunnel testing in ASCE 7, provides the detailed requirements. These are also discussed in Kopp (2023). There are a few approaches available, and more research is needed to understand the differences between them. The distinction between the aerodynamic coefficients obtained by direct measurements (see, e.g., Banks, 2011, 2013) and the loads obtained via correction of the wind speeds should be emphasized. For example, Asghari-Mooneghi et al. (2016) developed a method to probabilistically account for changes in the aerodynamic loads caused by changes in turbulence scale while Guo et al. (2021) developed a method to account for changes in turbulence intensity and scale.

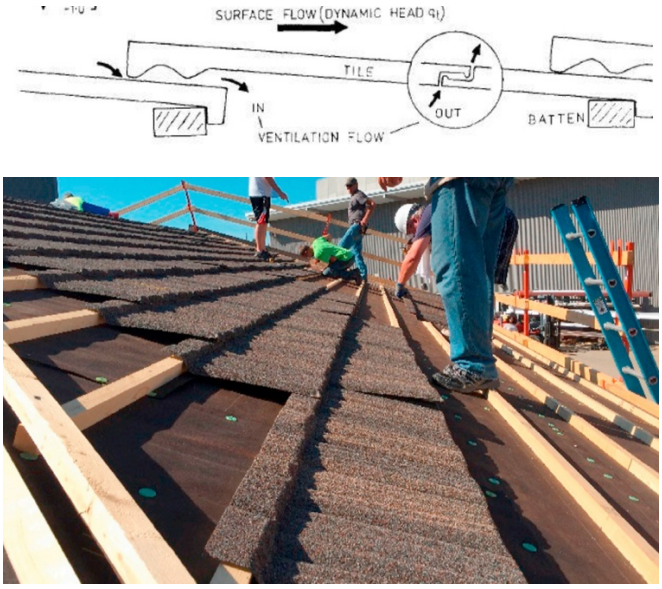

Figure 5. (Top) Small gaps between roof tiles that are important for new wind loads (from Smith, 2014). (Bottom) Photo of an air-permeable, multiplayer, discontinuous metal roof system (from Miller et al., 2020).

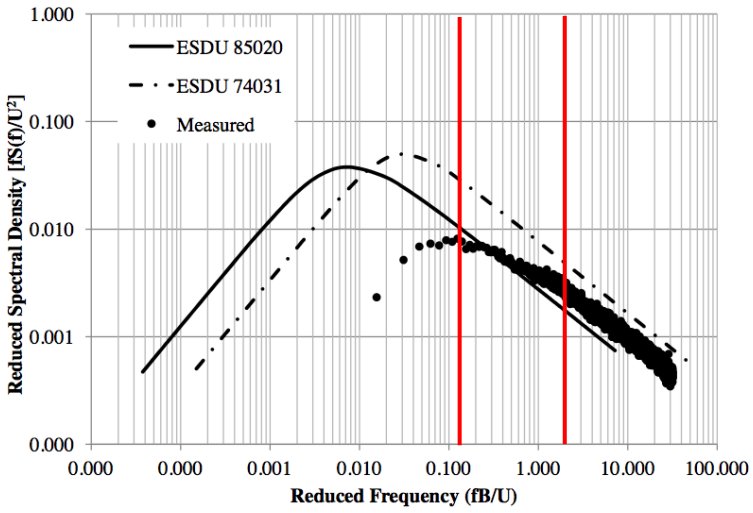

Figure 6. Velocity spectra used in a Partial Turbulence Simulation with a length scale of 1/20. The vertical red lines indicate approximately the bounds required by PTS (adapted from Stenabaugh et al., 2015).

At its core, PTS also relies on quasi-steady theory (QST) being able to account for the effects of the large-scale turbulence fluctuations. It essentially implies that the pressure fluctuations follow the upstream velocity fluctuations with a linear relationship (Holmes, 2015). When this occurs, the aerodynamic admittance function,

$$\chi^2(f) = 4\frac{U^2}{\bar{p}^2}\frac{S_p(f)}{S_u(f)}$$

has a value of unity. When this is the case, the aerodynamic load can be obtained by adjusting the wind speeds to account for changes in scale. QST tends to hold for area-averages in regions of separated flow (see the discussion in Wu and Kopp, 2019, and analysis by Wang and Kopp, 2022). While QST does not tend to hold for point pressures (e.g., Wang and Kopp, 2022), it tends to work well for area-averages (Wu and Kopp, 2016; Guo et al., 2021). However, the boundaries for appropriate areas have not yet been established. Based on the discussion above, this should consider relative areas, i.e., A_e/H^2.

For areas and spatial positions on the roof where QST holds, Guo et al. (2021) developed a method to take advantage that the fact that for turbulence levels typical of open and suburban terrains, the aerodynamic mechanisms and resulting quasi-steady coefficients are constant (Akon and Kopp, 2018; Wu and Kopp, 2018). For this, Guo et al. (2021) split the pressure coefficient fluctuations into two parts: a quasi-steady portion and the local portion, which is due to the body-generated turbulence effects, i.e.,

$$\Delta p(t) = \frac{1}{2}\rho V_s(t)^2 Cp(\theta,\beta) + p_{local}$$

where p_{local} is normalized based on the turbulence intensity in the PTS range, i.e.,

$$R = \frac{p_{local}}{0.5\rho \times |Cp(\theta,\beta)|(k_t^* + k_b^*)\overline{|V|^2}}$$

The distribution of the normalized local pressure coefficient is reasonably independent of terrain, as shown in Figure 7, area, wind direction, and position on the roof within the region the separated flow (Guo et al., 2021).

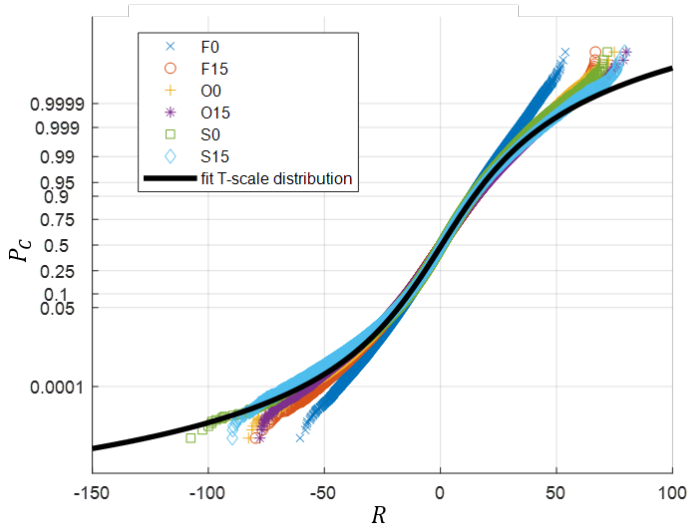

Figure 7. Cumulative distribution function of non-dimensional local pressure coefficient, *R* (Guo et al., 2021).

Using the quasi-steady coefficients and the statistical model for the local pressure coefficients, Guo et al. (2021) use a Monte-Carlo simulation approach to estimate the peak area-averaged pressures for

other terrains with different values of integral scale and turbulence intensity. Figure 8 shows one example, for one particular area on the roof for one wind direction is one terrain. Further work is needed to examine how this method works on buildings with other shapes and, particularly, how the local pressure coefficient, *R*, changes in these environments. While Guo (2021) has shown that the model is robust for hip and gable roofs, such models have not been attempted for air-permeable cladding systems.

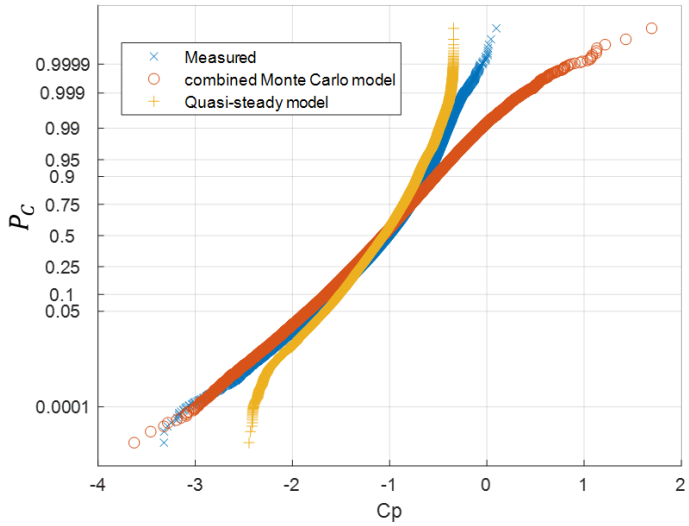

Figure 8. Comparison of the cumulative distribution functions of the area-averaged pressure coefficients, Cp, for C-16 from the measured data, the QS model, and the combined Monte-Carlo model in a suburban terrain with a nominal direction of 85° (from Guo et al., 2021).

5. Conclusions

The development of design wind loads for cladding systems and building components, particularly for those that are air-permeable with multiple layers, pose many challenges for wind engineers. This has necessitated the development of new tools and methods to improve performance-based design, on the one hand, and mitigate losses in severe wind storms, on the other. Recent developments in the understanding of turbulence and building geometry effects on the aerodynamics and surface pressure fields for the separated and reattaching flows near building edges has enabled a significant increase in the possibilities to develop such tools.

Consideration of the nature of the flow fields in regions of separated flows suggests that external pressure distributions could be presented as a function of non-dimensional area since a cladding panel of one size will experience different loads based on the size of the building. For low-rise building roofs, it appears that normalizing the area by the roof height squared may be reasonable. This approach has already been implemented for roof-mounted solar arrays, so there is already some experience with this in practice. However, further studies with high resolution pressure tap layout on both smaller and larger buildings would be useful.

From a wind tunnel testing perspective, small elements in cladding systems such as air and drainage gaps and air flow between multiple layers in roof and wall systems, ensure that it is practically impossible to accurately model these details at the typical scales of boundary layer wind tunnels. As a result, larger models are often used which cause violations of scaling laws and complete similarity of the model and prototype wind field simulations. Detailed studies of the aerodynamic mechanisms has indicated that partial turbulence simulations are valid and useful. Additional research has suggested that significant terrain corrections are possible if the wind tunnel tests capture the active scales of the

small-scale turbulence. However, further studies for a larger range of building and cladding geometries are still needed, particularly those that push the boundaries to provide a better understanding of the limitations.

As a final comment, it appears that complex non-stationary non-synoptic wind fields such as tornadoes will also require aerodynamic models for use in design. In fact, such models were used in the development of the tornado load provisions in ASCE 7-22 (2022). Having a clear understanding of how the details of the wind field alter the aerodynamic coefficients will be important so that the existing wealth of aerodynamic data for buildings in the atmospheric boundary layer can be examined – and potentially modified – for use in non-synoptic wind storms. Such an analysis has been done for one building by Kopp and Wu (2020), who showed how the streamline curvature in a high-swirl-ratio tornado wind field altered the aerodynamic loads using the same quasi-steady model as Guo et al. (2021).

References

Akon, A.F., Kopp, G.A., 2016. Mean pressure distributions and reattachment lengths for roof-separation bubbles on low-rise buildings. *J. Wind Eng. Ind. Aerodyn.* 155:115-125.

Akon, A.F., Kopp, G.A., 2018. Turbulence structure and similarity in the separated flow above a low building in the atmospheric boundary layer. *J. Wind Eng. Ind. Aerodyn.* 182:87-100.

American Society of Civil Engineers (ASCE), 2017, "Minimum design loads and associated criteria for building and other structures", ASCE 7-16, Reston, VA, USA.

American Society of Civil Engineers (ASCE), 2021, "Wind tunnel testing for buildings and other structures", ASCE 49-21, Reston, VA, USA.

American Society of Civil Engineers (ASCE), 2022, "Minimum design loads and associated criteria for building and other structures", ASCE 7-22, Reston, VA, USA.

Asghari-Mooneghi, M., Irwin, P., Gan Chowdhury, A., 2016. Partial turbulence simulation method for predicting peak wind loads on small structures and building appurtenances. *J. Wind Eng. Ind. Aerodyn.* 157:47–62.

ASTM D3679, 2013, "Standard specification for rigid poly vinyl chloride (PVC) siding", West Conshohocken, PA, USA.

ASTM D5206, 2013, "Standard test method for windload resistance of rigid plastic siding", West Conshohocken, PA, USA.

Banks, D., 2011. Measuring peak wind loads on solar power assemblies. Proc. 13th Int. Conf. Wind Eng., Amsterdam.

Banks, D., 2013. The role of corner vortices in dictating peak wind loads on tilted flat solar panels mounted on large, flat roofs. *J. Wind Eng. Ind. Aerodyn.* 123: 192-201.

Banks, D., Meroney, R.N., 2001, The applicability of quasi-steady theory to pressure statistics beneath roof-top vortices, *J. Wind Eng. Ind. Aerodyn.* 89:569-598.

Cherry, N.J., Hillier, R., Latour, M.E.M.P., 1984. Unsteady measurements in a separated and reattaching flow. *J. Fluid Mech.* 144:13.

Doddipatla, L.S., Wu, C.-H., Kopp, G.A., 2022. Wind loads on a 50m high, low-rise-shaped building with a flat roof. *Proc. 14th Americas Conf. Wind Eng.*, Lubbock, TX, USA.

Engineering Science Data Unit (ESDU), 1983, "Strong winds in the atmospheric boundary layer, Part 2: Discrete gust speeds", ESDU 83045. London.

Guo, Y., 2021, "A partial-turbulence approach to estimate peak wind loads on low-rise building roofs", PhD thesis, Western University, London, ON, Canada.

Guo, Y., Wu, C.H., Kopp, G.A., 2021. A method to estimate peak pressures on low-rise building models based on quasi-steady theory and partial turbulence analysis. *J. Wind. Eng. Ind. Aerodyn.* 218:104785.

Gurley, K.R., Masters, F.J., 2011. Post-2004 hurricane field survey of residential building performance. *Nat. Haz. Rev.* 12(4):177-183.

Holmes, J.D., 2015, "Wind loading of structures", 3rd Edition, CRC Press Boca Raton, Florida, USA.

Irwin, P.A., 2008. Bluff body aerodynamics in wind engineering, *J. Wind Eng. Ind. Aerodyn.* 96 (6-7):701-712.

Kopp, G.A., 2014. Wind loads on low-profile, tilted, solar arrays placed on large, flat, low-rise building roofs. *J. Struct Eng.* 140:04013057.

Kopp, G.A., 2023. Updates to the wind tunnel method for determining design loads in ASCE 49-21. *Wind Struct.* (submitted).

Kopp, G.A., Morrison, M.J., 2018. Component and cladding wind loads for low-slope roofs on low-rise buildings. *J. Struct. Eng.* 144(4):04018019.

Kopp, G.A., Wu, C.-H., 2020. A framework to compare wind loads on low-rise buildings in tornadoes and atmospheric boundary layers. *J. Wind Eng. Ind. Aerodyn.* 204:104269.

Lander, D.C., Letchford, C.W., Amitay, M., Kopp, G.A., 2016. Influence of the bluff body shear layers on the wake of a square prism in a turbulent flow. *Phys. Rev. Fluids* 1(4):044406.

Lander, D.C., Moore, D.M., Letchford, C.W., Amitay, M., 2018. Scaling of square-prism shear layers. *J. Fluid Mech.* 849:1096-1119.

Lin, J.X., Surry, D., 1998. The variation of peak loads with tributary area near corners on flat low building roofs. *J. Wind Eng. Ind. Aerodyn.* 77-78:185-196.

Liu, Y., Kopp, G.A., Chen, S.F., 2019. Effects of plan dimensions on wind loads for high-rise buildings. *J. Wind Eng. Ind. Aerodyn.* 194:103980.

Melbourne, W.H., 1979. Turbulence effects on maximum surface pressures – A mechanism and possibility of reduction. *Proceedings 5th International Conference on Wind Engineering*. Fort Collins, CO, USA, 541-551.

Miller, C.S., Kopp, G.A., Morrison, M.J., Kemp, G., Drought, N., 2017. A multichamber, pressure-based test method to determine wind loads on air-permeable, multilayer cladding systems, *Front. Built Env.* 3:7.

Miller, C.S., Kopp, G.A., Morrison, M.J., 2020, Aerodynamics of air-permeable multilayer roof cladding, *J. Wind Eng. Ind. Aerodyn.* 207:104409.

Morrison, M.J., Kopp, G.A., 2018. Effects of turbulence intensity and scale on surface pressure fluctuations on the roof of a low-rise building in the atmospheric boundary layer. *J. Wind Eng. Ind. Aerodyn.* 183:140-151.

Pratt, R.N., Kopp, G.A., 2014. Velocity field measurements above the roof of a low-rise building during peak suctions. *J. Wind Eng. Ind. Aerodyn.* 133:234-241.

Saathoff, P.J., Melbourne, W.H., 1997. Effects of free stream turbulence on surface pressure fluctuations in a separation bubble, *J. Fluid Mech.* 337:1-24.

Smith, D.J., 2014, "The wind resistance of clay and concrete roof tile systems", PhD thesis, University of Florida, Gainesville, FL, USA.

Sparks, P.R., Schiff, S.D., Reinhold, T.A., 1994. Wind damage to envelopes of houses and consequent insurance losses. *J. Wind Eng. Ind. Aerodyn.* 53(1-2):145-155.

Stenabaugh, S.E., Iida, Y., Kopp, G.A., Karava, P., 2015. Wind loads on photovoltaic arrays mounted on sloped roofs of low-rise buildings, parallel to the roof surface. *J. Wind Eng. Ind. Aerodyn.* 139:16-26.

Szilagyi, N., 2022. "Effective wind areas for the design of roof sheathing under wind loading", MESc thesis, Western University, London, ON, Canada.

Wang, J., Kopp, G.A., 2021. Comparisons of aerodynamic data with the Main Wind Force Resisting System provisions of ASCE 7-16 Part I: low-rise buildings. *J. Struct. Eng.* 147(3):04020347.

Wang, J., Kopp, G.A., 2022. Gust effect factors for regions of separated flow around rigid low, mid, and high-rise buildings. *J. Wind Eng. Ind. Aerodyn*. 232:105254.

Wu, C.H., Kopp, G.A., 2016. Estimation of wind-induced pressures on a low-rise building using quasi-steady theory. *Front. Built Env.* 2:5.

Wu, C.H., Kopp, G.A., 2018. A quasi-steady model to account for the effects of upstream turbulence characteristics on pressure fluctuations on a low-rise building. *J. Wind Eng. Ind. Aerodyn.* 179:338-357.

Wu, C.H., Kopp, G.A., 2019. Examination of the physical assumptions of a quasi-steady vector model using the integral momentum equation. *J. Wind Eng. Ind. Aerodyn.* 187:73-84.